

# CAVITATION IN A TRANSPARENT REAL SIZE VCO INJECTION NOZZLE

**Miranda R.<sup>1</sup>, Chaves H.<sup>1</sup>, Martin U.<sup>1</sup> and Obermeier F.<sup>1</sup>**

1. Institut für Mechanik und Fluidodynamik  
TU Bergakademie Freiberg, Germany

Due to the complex geometry of “valve covers orifice” (VCO) nozzles, details of the cavitation process in real size nozzles are very difficult to observe. Therefore, in the present investigation the tip of a standard VCO nozzle has been replaced by a glass prism which has a conical recess for the needle tip and two opposing holes of about 1 mm in length and 0.3 mm in diameter. Diesel fuel is mixed with  $\alpha$ -methylnaphthalene to match the index of refraction of the glass prism. This allows to observe the flow within the nozzle hole and at the needle seat for a real size injector geometry although these surfaces are curved and would normally deflect the light and distort the images. In a second step also the tip of the needle is replaced by one made of glass. Furthermore, by submerging the injector into the fuel mixture all distortions caused by the mismatch of the glass or fuel to the surrounding fluid can be eliminated, it allows observation from any view direction. In the actual experiments the needle has to be fixed at a pre-set lift because otherwise the closing impact of the needle would destroy the glass prism. The lift value is varied from 97  $\mu\text{m}$  up to full lift. Both the injection and the chamber pressure are varied to cover the complete range of cavitation numbers present in Diesel injectors. However, to avoid breakage of the glass prism the actual injection pressure and, hence, the flow velocity have to be chosen lower than those present in real injection systems. Back lighted pictures of the flow showing the location of cavitation in a side view of the nozzle holes as well as at the nozzle exit plane were illuminated by a 400 ns flash from a high efficiency LED. The primary role of the cavitation number for determining the flow behaviour is confirmed. The extent of the cavitation within the nozzle hole is determined by its dynamics only. For increasing cavitation numbers the cavitation region increases in length and eventually reaches out of the hole where it collapses. At the exit plane of the hole a strong vortical motion of the cavitation is found. At this point it has the shape of a filament or a string.

## 1. Introduction

It is well established that the atomization process of diesel fuel injected into an engine is initiated by flow perturbations especially by cavitation within the nozzle hole. During the opening and closing transient at very low lift values cavitation could also appear at the gap between the needle and the seat.

Visualization of the cavitating flow within “valve covers orifice” VCO nozzles has been performed up to now by many researchers in scaled-up models only, see e.g. [1, 2]. With two exceptions no observations in real size VCO nozzles have been published. In the first case Arcoumanis et al. [3] replaced one of the holes of a real size six hole VCO nozzle by a

perforated piece of glass, that allowed to observe the flow within the hole for a submerged injector and later by Miranda et al. [4] used the same technique to observe both the internal and external flow but for injection into atmospheric conditions. One of the conclusions of Arcoumanis et al. [3] is that the most important parameter characterizing the internal flow is the cavitation number but that the dynamics of the individual cavitation bubbles also plays a role. However, the dynamics of the bubbles cannot be scaled up. In spite of this there is a similarity of the flow in real size and scaled-up models of the same injector geometry. The open question is whether or not it is possible to manufacture real size transparent VCO injectors that in a later stage would permit the application of measurement techniques originally used for scaled-up models.

## 2. Experimental System

The core of the experimental set-up is the transparent nozzle. Figure 1 shows schematically the geometry of this nozzle from the view directions investigated in the experiments.

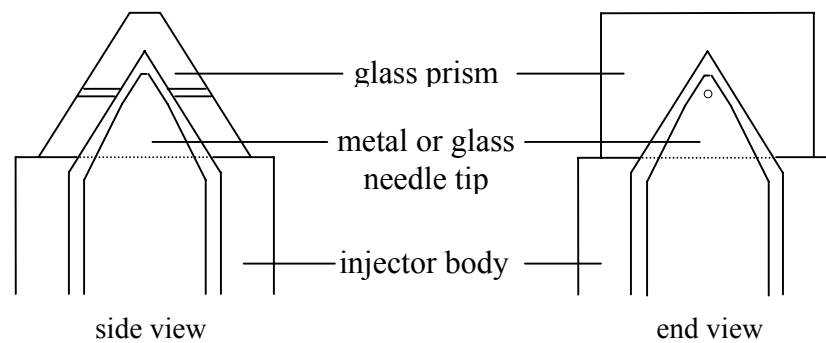


Fig. 1: Cross-sections through the injector tip with glued transparent nozzle.

Figure 2 is a picture of the injector with the nozzle and the needle. Here a needle with a glass tip is shown.

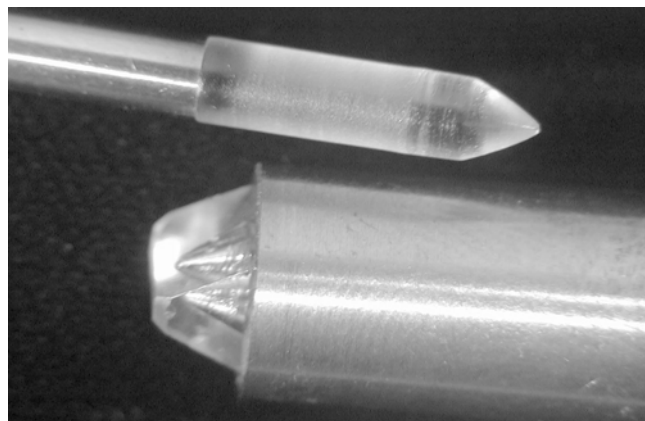


Fig. 2: Photograph of the injector tip with transparent nozzle and the needle with glass tip.

The needle was fixed at a preset lift value, since the needle would destroy the transparent nozzle during the closing process. Figure 3 and 4 show pictures of the transparent nozzle from two perpendicular directions displaying the exact geometry and the position of the needle relative to the seat. The field of view is 4.8 mm x 3.525 mm. One realizes that the needle is not symmetric to the seat. This is not a result of a misplaced needle but the result of movement of the prism during the curing of the glue which fixes and seals the prism onto the

injector body. The nozzle is a hand made product and this is the first successful example. As a result of this one can observe that the inlet corner of both holes is very slightly chipped which actually means that this corner is very sharp and that the holes are somewhat different in length. The one on the left has a length of 1.11 mm the other has a length of 0.96 mm. In both cases the diameter is 0.3 mm. The outlet of the hole on the right hand side is also chipped but this has only the effect of reducing the effective length of the nozzle hole. Figure 4 shows the case of a glass needle tip. This set-up allows to take pictures from an end side view. The image of the holes is not very sharp because in this case the microscope lens has been focused on the outline of the needle. The small depth of field of the microscope is used here to distinguish structures at different positions along the line of sight. The circular patterns are refractive index gradients in the glass. On the bottom right there is a small flaw which has resulted from the effects of pressure.

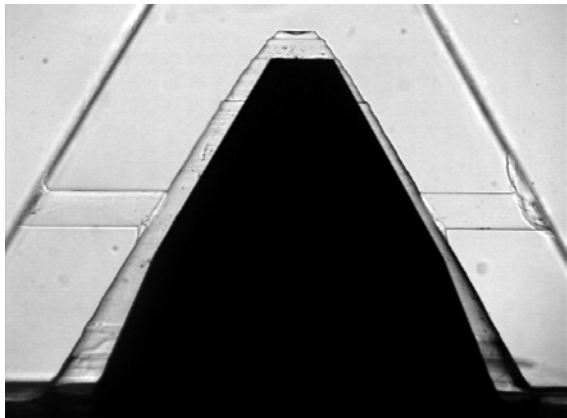


Fig. 3: Side view of the transparent nozzle with a metal needle tip

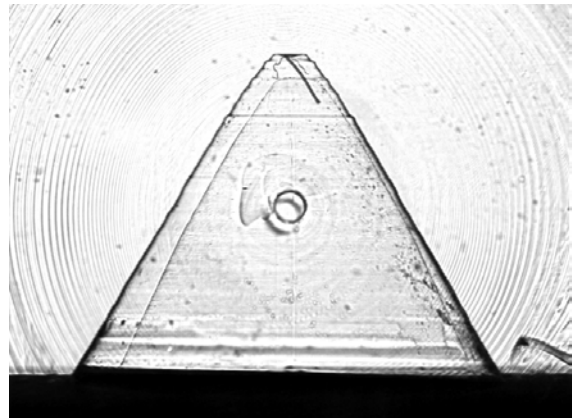


Fig. 4: End view of the nozzle with a glass needle tip

The flow is observed with a CCD camera and a long distance microscope. The images are back-lighted by a short light flash of 400 ns duration from a high efficiency LED. The repeatability of the light intensity from LEDs is extremely high, whereas spark sources suffer from large variations in intensity. The flow velocity is low due to the limited range of injection pressures applicable to the glass nozzle and, therefore, 400 ns are sufficient to “freeze” the pictures.

For injection into air it is normally not possible to obtain sharp images of both the internal and external flow simultaneously. This is due to the small depth of field of the optics and due to the difference in length of the optical path for the light propagating through the transparent nozzle and the light traversing the spray region (air). In the present case the injector was submerged in a chamber filled with the fuel. The refractive index of the diesel fuel was matched at the wavelength of the LED (630 nm) to the refractive index of the nozzle by adding about 40% by mass of  $\alpha$ -methylnaphthalene. This liquid has a higher index of refraction than both the glass and diesel fuel. It is an aromatic compound which has been used as a representative for aromatics in model Diesel fuels, [5]. The mixture has a somewhat higher density than ordinary Diesel fuel whilst the viscosity and surface tension are in the same range.

The remaining set-up consists of the injection chamber which is equipped with two opposing glass windows, a low pressure injection system composed of a fuel reservoir, which is pressurized by nitrogen, a fuel line, which is interrupted by a magnetic valve connected to the injector, and pressure transducers to monitor both chamber  $P_{ch}$  and injection pressure  $P_{inj}$ .

### 3. Experimental procedure

The experiment is started by the opening of the magnetic valve for 500 ms since the injector is always open. Pictures are taken after the opening transients have decayed (ca. 40 ms, steady state conditions). The chamber pressure downstream of the magnetic valve is monitored and is used as a trigger signal to start the picture acquisition. During the experiment the injection pressure remains constant. The chamber pressure increases slowly due to the influx of fuel into the chamber. The speed at which the chamber pressure rises is controlled by a small gas reservoir connected to the chamber. If the gas volume contained in this reservoir is small in comparison to the total volume of the injection chamber plus gas reservoir the pressure rise is very rapid. A large gas reservoir results in a slow increase. The net result is a variation of the cavitation number during one run.

The framing rate is 25 Hz giving a series of 14-15 pictures for each run. First picture is obtained within the opening transient and the last two-three are taken during the closing of the magnetic valve and the following pressure decay. The remaining eleven pictures taken during the quasi-steady conditions are evaluated.

### 4. Results and Discussion

Results are presented for cavitation numbers in the relevant range valid for injection and under steady state conditions. However, the corresponding Reynolds numbers are lower than those for real injection conditions due to the lower injection pressure permitted by the glass.

#### 4.1 Variation of the cavitation number

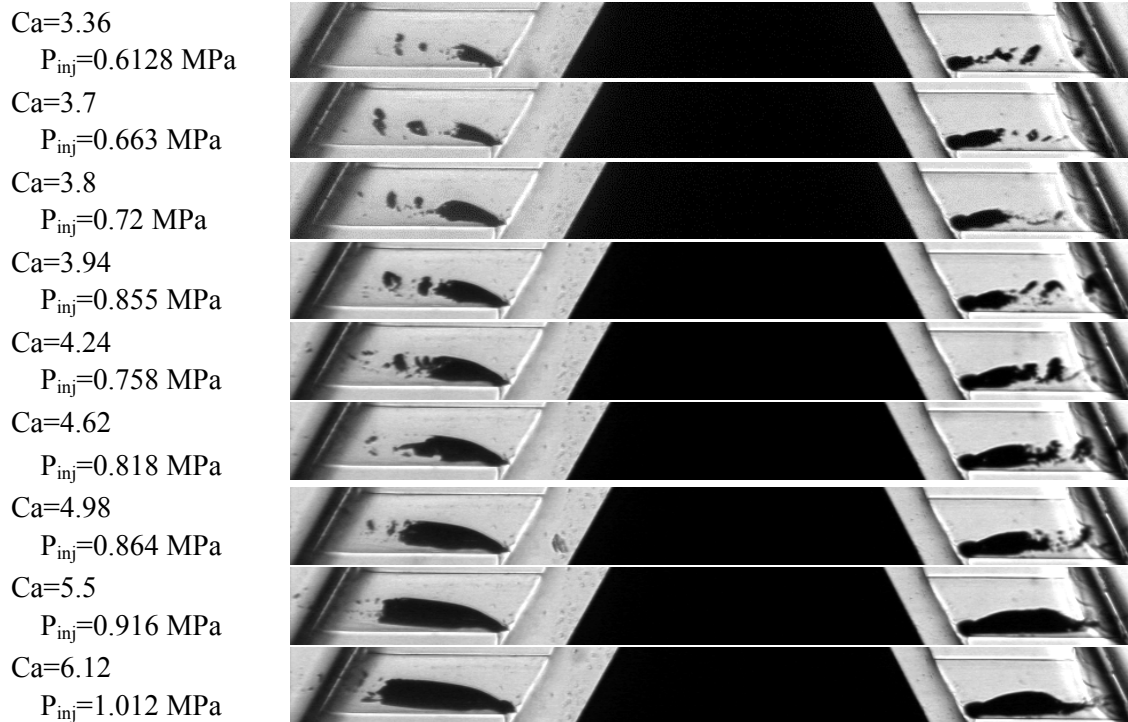


Fig. 5: Pictures of the flow in the injector for increasing cavitation number;  
field of view 4.8 mm x 0.425 mm

Figure 5 shows a series of pictures of the flow for increasing cavitation number defined by  $Ca = (P_{inj} - P_{ch}) / (P_{ch} - P_v) \approx (P_{inj} - P_{ch}) / P_{ch}$  since the vapor pressure  $P_v$  of the fuel is very small. Cavitation appears only in the holes so that only the part of the pictures which encompasses them is shown, compare with Figure 3. The gap between the seat and the metal needle is 310  $\mu m$  on the left hole and 175  $\mu m$  for the right one. Cavitation appears as black patches on the pictures. In spite of the differences in length and lift for these two holes, the cavitation extent and its behaviour are very similar. Cavitation starts at the lower inlet corner, which forces the inlet flow to turn by the largest angle. Its extent increases with cavitation number. The patch of cavitation attached to the inlet corner breaks up at its tip into smaller patches in a more or less regular manner. These patches are convected downstream and exit the nozzle holes. For a cavitation number larger than six cavitation reaches the exit of the shorter hole on the right hand side. The length of the cavitation is more or less independent of the length of the hole. This indicates that it is the dynamics of the cavitation which determines the location where it collapses or breaks up and not the geometry of the hole.

#### 4.2 Variation of needle lift

A further question concerns the effect of lift. To investigate the problem the preset lift of the needle is varied. Figure 6 shows two pictures taken at more or less the same cavitation number but for a different lift.

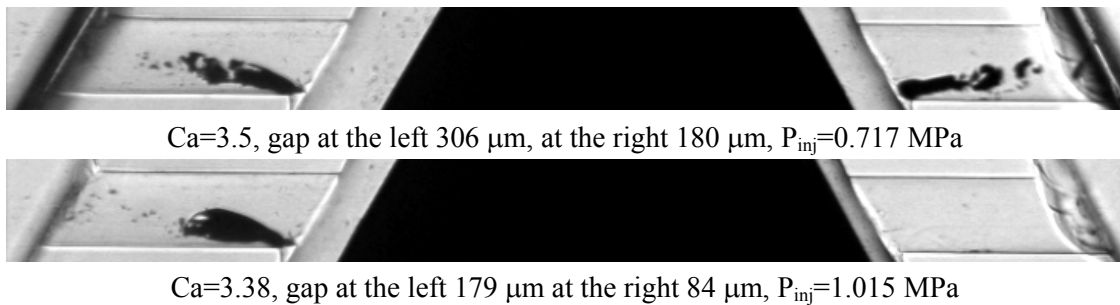


Fig. 6: Nozzle flow depending on the lift of the needle, field of view 4.8 mm x 0.425 mm.

Obviously, the gap between the needle and the seat is different for the two holes. The two pictures basically document the effect of lift we have observed. At low lift values cavitation is suppressed. This fact, which is the result of increased pressure losses at the seat, that effectively reduces the velocity and, therefore, the effective cavitation number. However, for larger cavitation numbers cavitation still appears but it is delayed in its appearance. Here, cavitation is not found at the seat.

#### 4.3 External flow and cavitation collapse

The cavitation number, at which the cavitation exits the nozzle, can be determined more easily when a different field of view is chosen. Figure 7 displays a range of cavitation numbers that reach a level comparable to those attained under engine operating conditions. Here only the left nozzle hole is shown. The collapse occurs outside of the nozzle and the length of the cavitating region enlarges with increasing cavitation number. Here it is emphasized that the cavitation numbers are achieved for varying injection pressures demonstrating that it is indeed the cavitation number that describes the flow behaviour for one particular nozzle hole.

For this nozzle hole cavitation reaches the exit in a form that has an effect on the nozzle effective area at a cavitation number of  $6.2 \pm 0.2$ . The area occupied by cavitation at the nozzle exit is a crucial value since it determines to a large extent the true exit velocity of the fuel. Most nozzles are characterized by an integral discharge coefficient. However, this does not allow to determine the real velocity, because the flow effective area is not known. The pictures shown here are line of sight pictures. This means that it is not possible to determine the position of the cavitation in a direction perpendicular to the plane of sight.

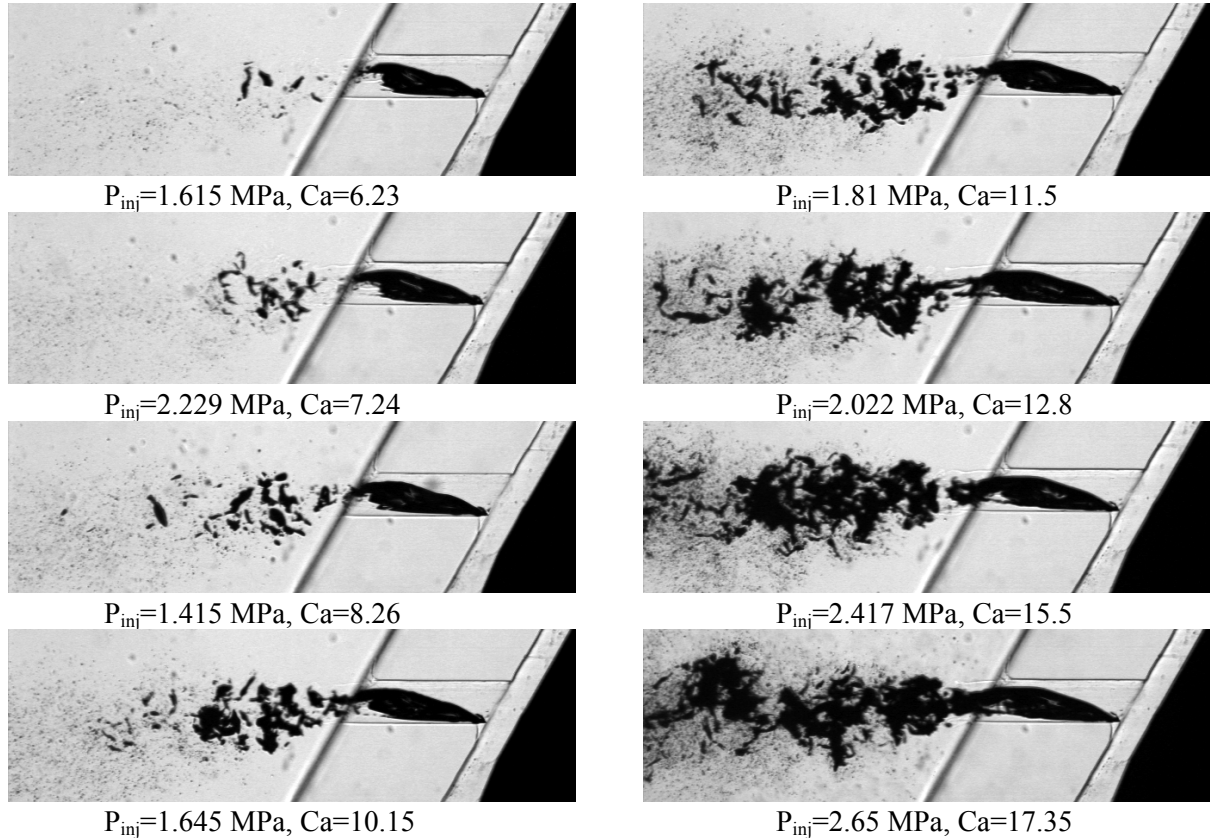
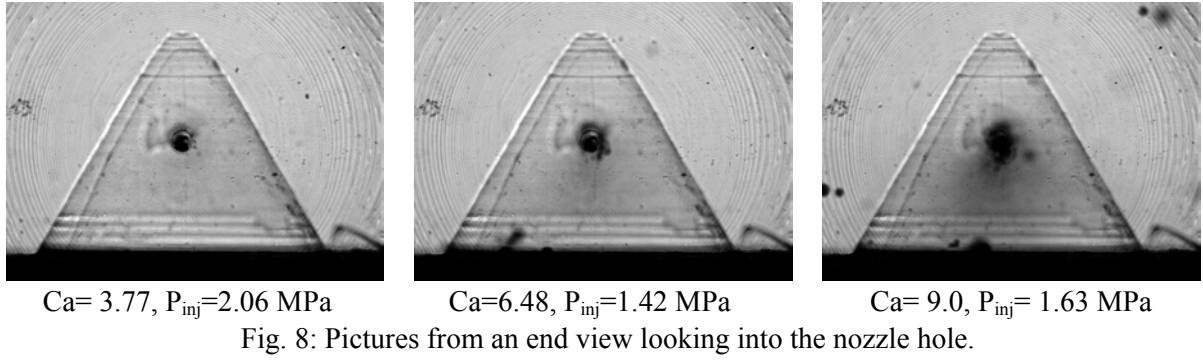


Fig. 7: Cavitation exiting the nozzle and collapsing in the chamber, field of view 4.26 mm x 1.29 mm

#### 4.4 End view into the nozzle hole

The use of a transparent needle now opens the possibility to measure the area and position of cavitation at the nozzle exit directly from a different view direction. By taking pictures from an end view, i.e. looking into the nozzle, and by focusing the microscope to the exit plane of the nozzle, it is possible to differentiate those structures that are sharp in this plane. Of course cavitation, which occurs behind this plane as well as between the exit plane and the lens, will obscure the view. The working range of this technique is limited by these effects as can be concluded from Figure 8. On these pictures the silhouette of the transparent needle is out of focus, compare with Figure 4. However, the field of view is too large to observe any details of the flow at the nozzle exit.

For a better observation of this area pictures of the flow were taken at even higher magnification, shown in Figure 9. The field of view is slightly larger than the hole diameter, ( $300 \mu\text{m}$ ), which corresponds more or less to the limit of resolution attainable by the microscope used.



In Figure 9 it is obvious that the flow has a rotation component in clockwise direction. This is well known from both large scale models as well as from numerical simulations. At the exit plane a thin filament of cavitation exits the nozzle. This type of cavitation has been called string cavitation in the literature, e.g. [3]. One realizes that the string becomes increasingly thicker with increasing cavitation number. Cavitation separates from the wall of the hole, as can be concluded from these pictures, and it follows a helical path as it exits from the nozzle.

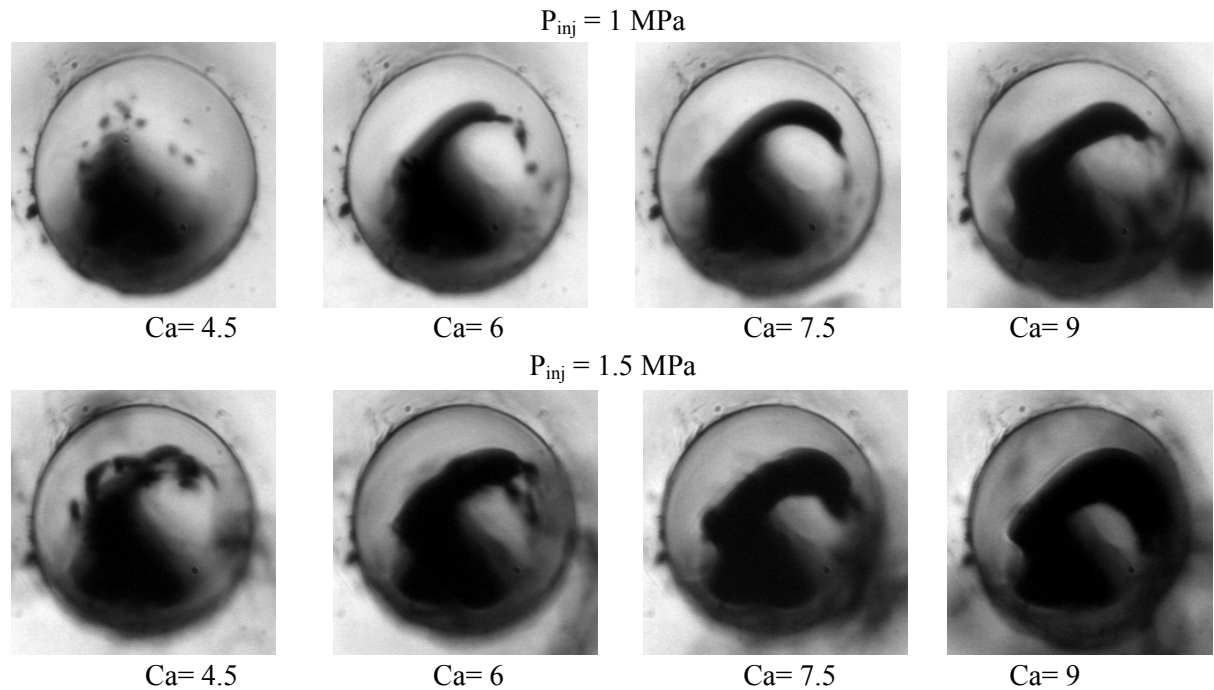


Fig. 9: Magnified view of the exit plane of the nozzle hole for various cavitation numbers and pressures.

Finally, it is of interest to get a first direct –still rough– estimate of the nozzle exit area occupied by cavitation. This is limited, however, by the ability to discriminate which structures are at the exit plane of the nozzle. Structures behind or in front of the focusing plane are not sharp, see the pictures for  $Ca=4.5$ . For a cavitation number above 7.5 one can see that a small part of the filament is well focused. For cavitation number higher than 9 it becomes increasingly difficult to observe the structures due to obscuration by those that are out of focus. At the point where the filament is well focused ( $Ca=9$ ) it has a diameter of about a fifth of the nozzle diameter giving an area of about 4% of the geometric nozzle area. To confirm this result it is tempting to use a light sheet in order to fix the plane from which the light would come. However, the light reaching the lens from such a plane would suffer the

same distortions produced by the cavitation which is present between the plane and the lens, Figure 7. By using contrast enhancement techniques and high pass filtering it may be possible to improve the resolution of the images also at higher cavitation numbers, but this has not been realized yet.

## 5. Conclusions

- It is possible to fabricate a real size transparent VCO nozzle.
- The nozzle can withstand pressure differences that allow to visualize the flow for realistic cavitation numbers.
- Cavitation appears at the sharp inlet at the position with the largest flow turning angle.
- Cavitation shows a dynamical behaviour independent of the hole length at least in the range investigated here. Therefore, it reaches the exit of a shorter hole at a lower cavitation number than for a long one.
- Cavitation forms as a compact patch, which at its tip breaks up into smaller patches more or less periodically.
- Once a certain limit is reached, cavitation exits the nozzle and collapses outside of the nozzle. With increasing cavitation number the length of the cavitating flow region increases for the submerged jet conditions presented here.
- Using a transparent needle the flow can be observed from a direction not easily realized otherwise.
- This technique opens the possibility to measure directly the area occupied by cavitation at the nozzle exit plane as well as its location within the plane for a limited range of cavitation numbers.

In summary the technique of a fully transparent VCO nozzle should allow to apply techniques that were developed for transparent, real size axial single hole nozzles, e. g. high resolution velocity measurements with cross-correlation, [6]. Together with pictures as they were presented here, the validation of numerical simulations of real size VCO nozzle flows should be possible. Finally, the future will show how restrictive the pressure limitations truly are, which were imposed on the experiments because of the use of glass nozzles.

## 6. References

- [1] Soteriou C C E and Andrews R J 1993 *Proc IMechE C465/051/93* 45-65
- [2] Laoonual T, Yule A J and Walmsley S J 2001 *Proc. ILASS-Europe 2001 Zürich*
- [3] Arcoumanis C, Badami M, Flora H and Gavaises M 2000 *SAE Paper 2000-01-1249*
- [4] Miranda R, Chaves H and Obermeier F 2002 *Proc. ILASS 2002, Zaragoza*
- [5] Hasse C and Peters N 2000 *SAE Paper 2000-01-2934*
- [6] Chaves H, Knapp M, Kubitzek A and Obermeier F 1995 *SAE Paper 950290*